The Formation of Ambiguity Functions with Frequency Separated Golay Coded Pulses

S.J. Searle, S.D. Howard, and W. Moran *Member, IEEE*

Abstract

Returns from radar transmitters are filtered to concentrate target power and improve SNR prior to detection. An ideal "thumbtack" filter response in delay and Doppler is impossible to achieve. In practice target power is distributed over the delay–Doppler plane either in a broad main lobe or in sidelobes with inherent limitations given by Moyal's identity. Many authors have considered the use of pairs or sets of complementary codes as the basis of radar waveforms. The set of filter outputs when combined reduces output to a thumbtack shape, at least on part of the delay–Doppler domain. This paper shows firstly that a pair of complementary codes cannot be multiplexed in frequency because of a phase difference which depends on the unknown range to any targets, thereby preventing the individual filter outputs from being combined coherently. It is shown that the phase term can be removed by multiplexing the second code twice, at offsets equally spaced above and below carrier, enabling the recovery of the sum of squared ambiguity functions. A proposed modification to the Golay pair results in codes whose squared ambiguities cancel upon addition. This enables complementary behaviour to be achieved by codes which are separated in frequency at the expense of introducing cross–terms when multiple closely separated returns are present. The modified Golay codes are shown to successfully reveal low power returns which are hidden in sidelobes when other waveforms are used.

Index Terms

Golay codes, Nonlinear filters, Radar signal processing, Signal design

I. Introduction

A radar system determines the range and velocity of reflectors in the environment by measuring the time delay and frequency shift on received pulses. The returned signal is match–filtered with the transmitted

S.J. Searle and W. Moran are with the University of Melbourne, Australia.

S.D. Howard is with the Defence Science and Technology Organisation, Australia.

signal at various frequency shifts, producing a delay–Doppler map. The ideal result of matched filtering is often described as a "thumbtack" shape; having a sharp response at the correct delay and Doppler, and being zero at all other locations. Mathematical constraints prevent this from ever happening. The best that one can achieve is to minimise the level of sidelobes or constrain their presence to particular areas of the delay–Doppler plane. This is problematic as weak returns may be masked if they occur in the sidelobes of much stronger returns.

Sidelobe suppression is often achieved by modulation of the radar pulse with a code sequence which is known to have favourable autocorrelation properties. The well known Barker code [1] is a binary code which results in minimal peak-to-peak range sidelobes. Polyphase codes (For example, Frank codes [2], P codes [3]) based on quadratic phase chirps have excellent range sidelobe properties.

While impossible to achieve an ideal "thumbtack" matched filter output with a single pulse, it is possible to at least approximate the ideal response on a region of the delay–Doppler plane with the use of "multiple" signals. Separate transmission and processing of an "up" chirp and a "down" chirp can clear up ambiguities related to Doppler sidelobes [4]. Robey et al [5] demonstrated how a radar beampattern could be viewed as a product of transmission and reflection beampatterns, and suggested design of signals such that the grating lobes of one beampattern did not line up with grating lobes in the other. This is an example of incoherent processing, since the sidelobe removal mechanism essentially relies on the magnitudes of the component beampatterns.

The generation of Composite Ambiguity Functions (CAF) [6] has been suggested as a means of coherently combining the returns from a set of waveforms in order to suppress sidelobes. The waveforms are chosen such that their respective ambiguity functions are out of phase and cancel completely upon addition except at the main lobe. The CAF relies upon the ability to transmit and process multiple waveforms independently of each other [6], [7] and then be able to coherently add the separate ambiguity functions together. To this end various methods of separation of the waveforms have been considered, including time and frequency separation [8] and also Walsh–Hadamard spreading [9]. Additionally, approximations to the CAF have been formed via frequency division multiplexing. However, this method relies on at least partial knowledge of the positions of the interfering targets and clutter[7]. In the case of frequency and time separation, computation of the CAF is hampered by the fact that each term in the CAF is affected by a phase factors which depends upon the unknown target range, the unknown target velocity or both[8], [6].

It can be shown that in the case of time separation the actual ambiguity function conincides with the CAF exactly along the zero–Doppler axis [8]. One can therefore achieve an ideal ambiguity func-

tion response along the zero–Doppler crossection (within delay limits) by time separation of a set of complementary coded waveforms. Suitable waveform sets include sets of 4 PONS waveforms [8] and complementary Golay pairs [10]. Golay pairs generally have poor Doppler tolerance, and this has discouraged their use in radar applications. It has recently been demonstrated [11] that pulse trains of Golay complementary waveforms can be given significant Doppler tolerance by appropriate choice of the ordering of the complementary waveforms within the pulse train.

One disadvantage of time separation is a limit on the measurable delay (beyond which range ambiguities occur). This limit can be extended by increasing the separation of pulses. However the requirement that the target maintains a relatively constant range and velocity over the interval and the total energy on target is better served by a shorter time period. Another disadvantage is that multiple PRIs must pass before the range-Doppler map can be constructed. Large sets of complementary functions can thus take an inordinately long time to process when separated in time.

The major advantage of choosing to separate the complementary/orthogonal waveforms in frequency is that it allows a result to be obtained on a pulse by pulse basis, rather than needing a pulse train. However due to the aforementioned target range dependent phase factors it is impossible to achieve coherent combination of the complementary waveforms with linear processing, e.g. bandpass and matched filtering, except at a finite number of known ranges.

This main purpose of this paper is to propose a method, based non-linear signal processing, for obaining detection statistics with CAF like properties for frequency multiplexed waveforms. The paper reviews the problems which occur when one attemps to approximate, even locally, a CAF with a set of frequency or time multiplexed phase code modulated pulses. Issues which must be resolved in order to obtain a detection statistic with CAF like properties are discussed. A frequency multiplexing scheme which enables the recovery the square of individual pulse ambiguity functions with complete cancellation of target range dependent phases is presented. For our scheme to be effective, in terms of constructing CAF like detection statistics for multiplexed complemetary waveform, it was necessary to find waveforms which are complementary in the squares of their autocorrelation functions. A technique for constructing polyphase code pairs of such waveforms from conventional Golay complementary waveforms is developed. Overall our method enables sidelobe free ranging of stationary targets via frequency multiplexing of complementary waveforms. No special assumptions are made; standard assumptions like the complex radar cross section of a target being constant over a small frequency range are implicit. Although this method is intended for use in clutter–limited scenarios, the effect of noise on the method is examined by a Monte Carlo ROC analysis and compared with matched filter detection.

II. Signal Model

Let p be a sequence of N elements each having unit amplitude, and autocorrelation sequence $R_p(k)$. This sequence is used to modulate a series of pulses, thus forming a baseband signal b for use in pulse compression radar.

$$b(t) = \sum_{n=0}^{N-1} p_n \Omega(\frac{t}{T_c} - n - 0.5) \tag{1}$$

where Ω is a pulse shaping function having support mostly confined to $(-0.5, 0.5)$.

$$\int_{-0.5}^{0.5} \Omega(t)^2 \approx 1 \tag{2}$$

and T_c is the chip length in seconds. The ambiguity function of b, $\chi_b(\tau, \phi)$, is defined as

$$\begin{aligned} \chi_b(\tau, \phi) &= \int_{-\infty}^{\infty} b(t) b^*(t+\tau) e^{i\phi t}\, dt \\ &= T_c \sum_{k=\infty}^{\infty} R_p(k, \phi T_c) \chi_\Omega(k - \frac{\tau}{T_c}, \phi T_c) \end{aligned} \tag{3}$$

Since $\Omega(t)$ has limited support, this can be further expressed as

$$\chi_b(\tau, \phi) = T_c \left[\chi_\Omega(k_1(\tau) - \frac{\tau}{T_c}, \phi) R_p(k_1(\tau), \phi T_c) + \chi_\Omega(k_2(\tau) - \frac{\tau}{T_c}, \phi) R_p(k_2(\tau), \phi T_c) \right] \tag{4}$$

where

$$k_1(\tau) = \left\lceil \frac{\tau}{T_c} \right\rceil - 1 \tag{5}$$

and

$$k_2(\tau) = \left\lceil \frac{\tau}{T_c} \right\rceil = k_1 + 1 \tag{6}$$

Here $R(k, \phi)$ refers to the discrete–time ambiguity function formed from a discrete sequence. At $\phi = 0$ this is equivalent to autocorrelation.

The baseband signal $b(t)$ is used to modulate a carrier of frequency ω_c and transmitted.

$$s(t) = b(t) e^{i\omega_c t} \tag{7}$$

It may be desirable to offset the signal in frequency by ω_f radians, and/or in time by T seconds. In this case the transmitted signal is

$$s_{ft}(t) = b(t - T) e^{i(\omega_c + \omega_f)t} \tag{8}$$

This signal is reflected from a target and returned to the receiver at t seconds after transmission. Assuming monostatic radar, it follows that the delay d between transmission and reception is approximately equal to

$$d(t) \approx \frac{2r_0 - 2vt}{c} \tag{9}$$

where v is the radial velocity of the target and r_0 is its distance from the transceiver. The received signal can thus be expressed as

$$\tilde{s}_{ft}(t) = Ab(t - T - d)e^{i(\omega_c+\omega_f+\psi)t}e^{-i(\omega_c+\omega_f)d} \tag{10}$$

where ψ is the frequency shift caused by the Doppler effect and is equal to

$$\psi = (\omega_c + \omega_f)\frac{2v}{c} \tag{11}$$

A is the complex attenuation factor inherent in the transmission & reflection process.

The received signal is subjected to a matched filter bank in order to determine the existence of a target at a given range and Doppler shift. This is equivalent to sampling the cross–ambiguity function of the transmitted and received signals.

$$\begin{aligned}\chi_{\tilde{s}_{ft}s_{ft}}(\tau,\phi) &= \int_{-\infty}^{\infty} \tilde{s}_{ft}(t)s^*_{ft}(t-\tau)e^{-i\phi t}\,dt \\ &= Ae^{i(\omega_c+\omega_f)(\tau-d)}e^{i(\psi-\phi)(T+d)}\chi_b(\tau-d,\phi-\psi)\end{aligned} \tag{12}$$

Note that the first phase factor depends upon the unknown delay to target d and transmitted frequency ω_c. The second phase factor depends on the unknown Doppler shift (and thus on carrier frequency $\omega_c + \omega_f$) and the total unknown delay. We remark that such phase terms are often glossed over in radar literature, being referred to as "of no consequence" [12] or simply ignored altogether [13], presumably being subsumed into the A factor.

When there is no offset in frequency or time then (12) devolves to

$$\chi_{\tilde{s}s}(\tau,\phi) = Ae^{i\omega_c(\tau-d)}e^{-i\phi(T+d)}\chi_b(\tau-d,\phi-\psi) \tag{13}$$

The cross–ambiguity of a signal shifted in time and frequency with an unshifted signal is

$$\chi_{\tilde{s}_{ft}s}(\tau,\phi) = Ae^{i\omega_c(\tau-d)}e^{i(\psi-\phi)(T+d)}e^{i\omega_f(T+d-d)}\chi_b(\tau-T-d,\phi-\psi-\omega_f) \tag{14}$$

III. Formation of Ambiguity Function from 2 multiplexed signals

The following discussion can be generalised to the case where there are more than two codes in the complementary set.

Let b_1 and b_2 be two continuous baseband pulse modulated sequences formed from two distinct discrete sequences p_1 and p_2. The first sequence undergoes carrier modulation at ω_c. The second also undergoes carrier modulation but offset from carrier by ω_f and delayed by T. The multiplexed signal s_m is thus

$$s_m(t) = b_1(t)e^{i\omega_c t} + b_2(t-T)e^{i(\omega_c+\omega_f)t} \tag{15}$$

The signal returned from a target at delay d is thus

$$\begin{aligned}\tilde{s}_m(t) &= Ab_1(t-d)e^{i\omega_c(1+\frac{2v}{c})t}e^{-i\omega_c d} + Ab_2(t-d-T)e^{i(\omega_c+\omega_f)(1+\frac{2v}{c})t}e^{-i(\omega_c+\omega_f)d} \\ &= Ab_1(t-d)e^{i(\omega_c+\psi_1)t}e^{-i\omega_c d} + Ab_2(t-d-T)e^{i(\omega_c+\omega_f+\psi_2)t}e^{-i(\omega_c+\omega_f)d}\end{aligned} \tag{16}$$

assuming that the separations in time and frequency are small enough that the attenuation coefficient A does not change. Note that the Doppler affecting each component is different, as the components are of differing frequency. The two Doppler terms are in this case

$$\psi_1 = \frac{2v}{c}\omega_c \tag{17}$$

and

$$\psi_2 = \frac{2v}{c}(\omega_c + \omega_f) \tag{18}$$

Note also that the delay in b_2 will be altered if v is nonzero. This time dilation effect is assumed to be negligible.

The cross–ambiguity function between transmitted and received signals is thus

$$\begin{aligned}\chi_{\tilde{s}_m s_m}(\tau,\phi) &= Ae^{i\omega_c(\tau-d)}e^{-i\phi(T+d)}\chi_{b_1}(\tau-d,\phi-\psi_1) \\ &+ Ae^{i\omega_c(\tau-d)}e^{-i(\psi_2-\phi)(T+d)}e^{i\omega_f(T+d-d)}\chi_{b_1b_2}(\tau-T-d,\phi-\psi_2-\omega_f) \\ &+ Ae^{-i\omega_c(\tau-d)}e^{i(\psi_1-\phi)(T+d)}e^{-i\omega_f(T+d-d)}\chi_{b_1b_2}(\tau+T+d,\phi+\psi_1+\omega_f) \\ &+ Ae^{i(\omega_c+\omega_f)(\tau-d)}e^{i(\psi_2-\phi)(T+d)}\chi_{b_2}(\tau-d,\phi-\psi_2)\end{aligned} \tag{19}$$

The second and third terms above are cross–terms which occur at offsets in time and frequency in the vicinity of the delays and frequency offset used in multiplexing. These cross–terms can be removed and discarded via truncation on the delay–Doppler plane.

$$\chi_{\tilde{s}_m s_m}(\tau,\phi) = Ae^{i(\omega_c(\tau-d)-\phi(T+d))}\left(\chi_{b_1}(\tau-d,\phi-\psi_1) + e^{i(\omega_f(\tau-d)+\psi_2(T+d))}\chi_{b_2}(\tau-d,\phi-\psi_2)\right) \tag{20}$$

In practice (20) will not be computed directly. Instead the two non–offset terms will be computed separately and combined. The received signal $\tilde{s}_m(t)$ is downmixed by ω_c, lowpass filtered and matched to b_1. It is also downmixed by $\omega_c + \omega_f$, lowpass filtered, delayed by T and matched to b_2. This has the advantage of removing time dependent carrier factors. The two processed signals are

$$\xi_0(\tau, \phi_1) = Ae^{-i(\omega_c d + \phi_1(T+d))}\chi_{b_1}(\tau - d, \phi_1 - \psi_1) \tag{21}$$

and

$$\xi_1(\tau, \phi_2) = Ae^{-i(\omega_c d + \phi_2(T+d))}e^{i(\psi_2(T+d) - \omega_f d)}\chi_{b_2}(\tau - d, \phi_2 - \psi_2) \tag{22}$$

In general these quantities cannot be combined since the Doppler shift differs at each frequency. It is necessary to translate the second ambiguity function along the frequency axis in order for the underlying χ_b functions to be aligned. For this to be the case,

$$\phi_1 - \psi_1 = \phi_2 - \psi_2 \tag{23}$$

which yields

$$\phi_2 = \phi_1 + \psi_1\frac{\omega_f}{\omega_c} = \phi_1 + \frac{2v}{c}\omega_f \tag{24}$$

The translated version of ξ_1 is thus

$$\xi_1(\tau, \phi_1 + \psi_1\frac{\omega_f}{\omega_c}) = Ae^{i(-\omega_c d - \phi_1(T+d))}e^{i(-\omega_f d + \psi_1(T+d))}\chi_{b_2}(\tau - d, \phi_1 - \psi_1) \tag{25}$$

and is coherently combined with ξ_0 to give $\tilde{\chi}(\tau, \phi)$, an approximation to the CAF $\chi_{\tilde{s}_m s_m}$ within time and bandwidth limitations.

$$\begin{aligned}\tilde{\chi}(\tau, \phi) &= \xi_0(\tau, \phi) + \xi_1(\tau, \phi + \psi_1\frac{\omega_f}{\omega_c}) \\ &= Ae^{i(-\omega_c d - \phi_1(T+d))}\left(\chi_{b_1}(\tau - d, \phi - \psi_1) + e^{i(-\omega_f d + \psi_1(T+d))}\chi_{b_2}(\tau - d, \phi - \psi_1)\right)\end{aligned} \tag{26}$$

Since the translation computation (24) requires the unknown target velocity v, it is not generally possible to translate the ambiguity surfaces such that the frequency separated components are properly aligned. Nevertheless as $v << c$ the required translation is small. One may be able to adequately approximate (26) by using $\xi_1(\tau, \phi_2)$ in place of the shifted version. This approximation essentially substitutes ψ_2 for ψ_1. The difference is $\omega_f\frac{2v}{c}$ which is relatively small.

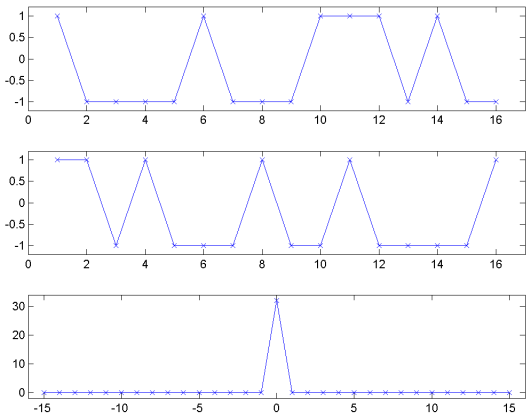

Fig. 1. Complementary Golay pair and sum of autocorrelation sequences

A. Complementary Golay pairs

A complementary Golay pair [10] is one possible choice for b_1 and b_2. A Golay pair is a pair of sequences whose autocorrelations add up to a delta function, illustrated in figure 1. The CAF of such a pair is characterised by a spike along the zero–Doppler axis. The width of this spike is equal to twice the chip length of the pulse code modulation, and its shape is dependent upon the underlying pulse shaping function.

Figure 2 presents a pulse code modulated Golay pair and their autocorrelation sum. Figure 3 is the

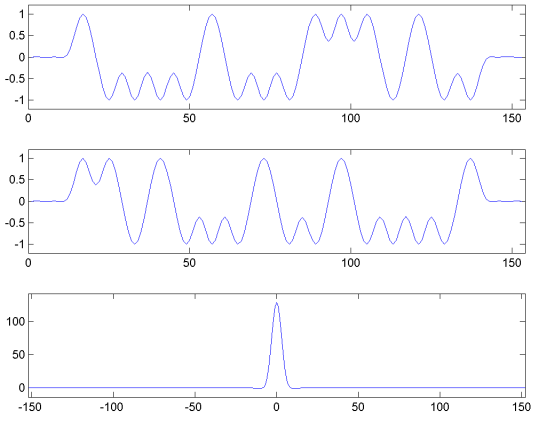

Fig. 2. Baseband Golay–coded signals and sum of autocorrelations

full ambiguity surface of the first baseband modulated Golay sequence, and figure 4 is the magnitude of the sum of the ambiguity functions. The zero–Doppler axis of these plots (i.e. delay–only) corresponds

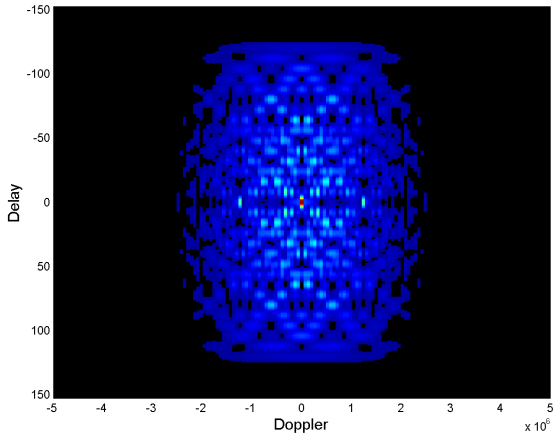

Fig. 3. Ambiguity surface of single baseband Golay signal

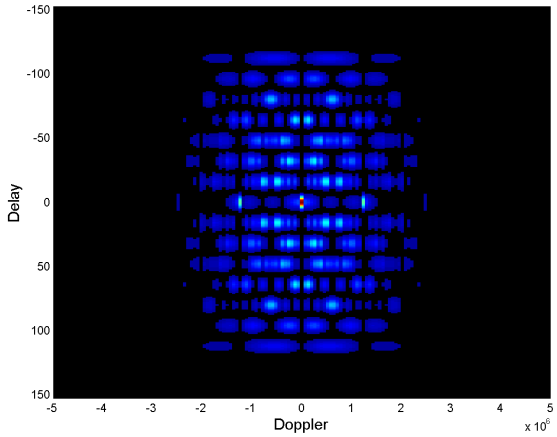

Fig. 4. Sum of ambiguity functions of baseband modulated Golay pair

to the autocorrelations of their respective signals. Observe that combination of the ambiguity surfaces only removes sidelobes along the zero–Doppler axis, although the off–axis power has been reduced. The exact sidelobe pattern produced in the CAF is a function of the Golay pair used.

B. Separation in time

It is evident from (26) that the combined ambiguity function generally cannot be achieved through the multiplexing of the component signals, due to the phase term which appears as the coefficient of the second component. This phase term depends upon the offset frequency ω_f and the Doppler frequency ψ_2. When both of these values are zero, the ambiguity function reduces to

$$\tilde{\chi}(\tau,\phi) = Ae^{-i[\omega_c d+\phi(T+d)]}\left[\chi_{b_1}(\tau-d,\phi)+\chi_{b_2}(\tau-d,\phi)\right] \tag{27}$$

If Doppler is known to be zero then the target is stationary and there is no point evaluating the above at values of ϕ other than zero. The equation further reduces to

$$\tilde{\chi}(\tau,0) = Ae^{-i\omega_c d}\left[\chi_{b_1}(\tau-d)+\chi_{b_2}(\tau-d)\right] \tag{28}$$

Thus it is possible to compute the ambiguity function at zero Doppler for stationary targets by multiplexing the individual waveforms via separation in time.

Figure 5 shows a baseband pulse code modulated Golay pair, separated in time by 500 samples. This signal is delayed by 200 samples and correlated with the original signal. The cross–correlation is maximised at a delay of 200. Sidelobes occur only at the PRI boundaries. The value of the cross–correlation within a PRI could be equivalently computed by processing the returns from each pulse separately and combining the results.

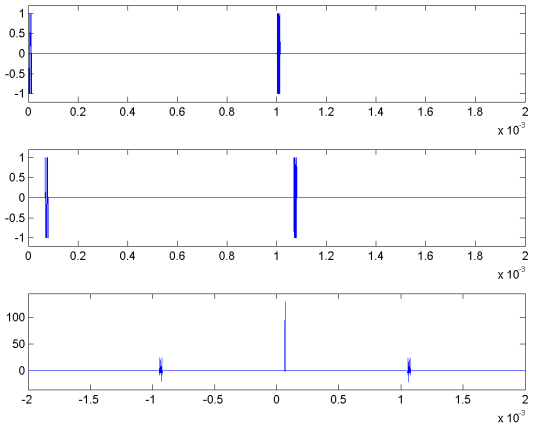

Fig. 5. Time separated Golay codes, delayed version, and their cross–correlation

C. Separation in Frequency

An advantage to separation in frequency is that target detection and ranging can be performed with a single pulse; one is not forced to wait for multiple PRIs in order to send the entire set of signals. Furthermore time sidelobes are replaced by frequency sidelobes, which is preferable if the targets are known to be stationary, or at least slow. However if frequency separation is performed then ω_f is nonzero and the phase coefficient then depends upon the unknown target delay d. It is thus not possible to compute the ambiguity function when frequency separation is used.

Figure 6 presents the cross–correlations of each frequency–separated Golay–coded signal with the original baseband signal. The two correlations have the same magnitude. However in this example when the correlations are combined, the offset phase terms cause the main lobes to interfere while the sidelobes are reinforced. It must be stressed that the effect upon combination is a function of offset frequency and target range.

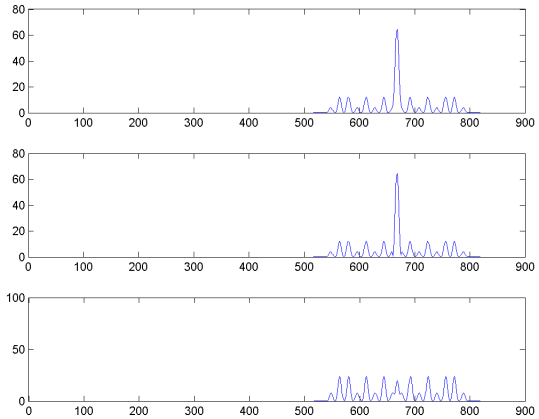

Fig. 6. Combination of cross–correlations of frequency–offset Golay–coded signals

1) Recovery of the square of the ambiguity function: Consider the second sequence of a frequency separated pair, which has been modulated at $\omega_c + \omega_f$. Consider the same sequence modulated below carrier by the same offset, i.e. at $\omega_c - \omega_f$. When demodulated and lowpass filtered, this signal component is processed with b_2 to form

$$\xi_{-1}(\tau, \phi) = Ae^{i[-\omega_c d - \phi(T+d)]} e^{i(\omega_f d + \psi_{-1}(T+d))} \chi_{b_2}(\tau - d, \phi - \psi_{-1}) \tag{29}$$

The difference in Doppler shift between ξ_1, ξ_{-1} and ξ_0 may be accounted for, giving

$$\xi_1(\tau, \phi_0 + \omega_f \frac{2v}{c}) = Ae^{i[-(\omega_c+\omega_f)d+(\psi_0-\phi_0)(T+d)]}\chi_{b_2}(\tau - d, \phi_0 - \psi_0) \tag{30}$$

and

$$\xi_{-1}(\tau, \phi_0 - \omega_f \frac{2v}{c}) = Ae^{i[-(\omega_c-\omega_f)d+(\psi_0-\phi_0)(T+d)]}\chi_{b_2}(\tau - d, \phi_0 - \psi_0) \tag{31}$$

and their product is

$$\xi_1(\tau, \phi_0 + \omega_f \frac{2v}{c})\xi_{-1}(\tau, \phi_0 - \omega_f \frac{2v}{c}) = A^2e^{2i(-\omega_c d+(T+d)(\psi_0-\phi_0))}\chi^2_{b_2}(\tau - d, \phi_0 - \psi_0) \tag{32}$$

As previously discussed, the absence of knowledge of the target velocity precludes the above computation. However since the target speed v is small with respect to the propagation velocity c, it may be approximated as

$$\begin{aligned}\xi_1(\tau, \phi_0 + \omega_f \frac{2v}{c})\xi_{-1}(\tau, \phi_0 - \omega_f \frac{2v}{c}) &\approx \xi_1(\tau, \phi_1)\xi_{-1}(\tau, \phi_{-1}) \\ &= A^2e^{2i(-\omega_c d-(\phi-\psi_0)(T+d))} \\ &\quad \times \chi_{b_2}(\tau - d, \phi - \psi_1)\chi_{b_2}(\tau - d, \phi - \psi_{-1})\end{aligned} \tag{33}$$

and combined with $\xi_0^2(\tau, \phi)$ to produce $\Upsilon(\tau, \phi)$

$$\begin{aligned}\Upsilon(\tau, \phi) &= \xi_0^2(\tau, \phi) + \xi_1(\tau, \phi) \times \xi_{-1}(\tau, \phi) \\ &\approx A^2e^{i2(-\omega_c d-(\phi-\psi_0)(T+d))}\left(\chi^2_{b_1}(\tau - d, \phi - \psi_0) + \chi^2_{b_2}(\tau - d, \phi - \psi_0)\right)\end{aligned} \tag{34}$$

In other words, the squares of the ambiguity functions of the component signals can be recovered and coherently combined if the waveform is multiplexed at an equal offset above and below carrier. Complementary behaviour can thus be achieved provided that the squares of the underlying code sequences are complementary.

In the particular case that the target velocity is known to be zero, the above approximation is exact. In this case Υ need only be computed along the zero–Doppler axis, and is

$$\Upsilon_0(\tau) = A^2e^{i2(\omega_c(\tau-d))}\left(\chi^2_{b_1}(\tau - d, 0) + \chi^2_{b_2}(\tau - d, 0)\right) \tag{35}$$

2) Modified Golay code pair: A complementary Golay pair is binary valued. The autocorrelation of a Golay sequence is thus real valued, and its square is positive. A Golay pair, or indeed any binary valued code pair, is thus not complementary in the square, since complementarity requires one of the squared autocorrelations to be the negative of the other. Such a code pair must necessarily be complex–valued.

If $g_1(n)$ and $g_2(n)$ form a Golay pair then by definition

$$R_{g_1}(k) + R_{g_2}(k) = 2N\delta(k) \tag{36}$$

where N is the length of the sequences. Observe that when $k \neq 0$,

$$R_{g_1}(k) = -R_{g_2}(k) \tag{37}$$

$$R^2_{g_1}(k) = R^2_{g_2}(k) \tag{38}$$

If the sequences are constructed in a standard manner and have length a power of 2, $N = 2^x$, then the two sequences are even–shift orthogonal [14], i.e.

$$R_{g_1}(2k) = R_{g_2}(2k) = 0, \quad \text{for } k \neq 0, \tag{39}$$

Define a new sequence $q(n)$ in terms of $g_2(n)$ as

$$q(n) = j(n)g_2(n) \tag{40}$$

where each $j(n)$ is a unit magnitude complex number. The autocorrelation sequence of $q(n)$ is thus

$$R_q(k) = \sum_n j(n)g_2(n)j^*(n+k)g_2^*(n+k) \tag{41}$$

If $j(n)$ is constrained to the form

$$j(n) = e^{ifn} \tag{42}$$

then the expression for R_q simplifies to

$$\begin{aligned} R_q(k) &= e^{ifk} \sum_n g_2(n)g_2^*(n+k) \\ &= j(k)R_{g_2}(k) \end{aligned} \tag{43}$$

The square of this is complementary with the autocorrelation of g_1 only if

$$j^2(k)R^2_{g_2}(k) = -R^2_{g_1}(k) \tag{44}$$

$$j(k) = \pm i \quad \text{for } k \text{ odd} \tag{45}$$

We do not especially care about the values of j for even k, since the autocorrelations of length 2^x Golay codes vanish at all nonzero even lags. However we also require $j(0) = 1$. The simplest expression for f which satisfies $j(0) = 1$ and (42) and (45) is to set $f = \frac{\pi}{2}$ yielding

$$j(n) = e^{i\frac{\pi}{2}n} \tag{46}$$

The binary code $g_1(n)$ and the four–phase code $q(n)$ thus form a pair whose squared autocorrelations are complementary. They may be used to modulate two frequency separated components of a radar signal in the manner described in the previous section.

Note that the formation of q relies only upon the original code g_2 having the same autocorrelation magnitude as g_1, and having zero valued autocorrelation at even valued lags. One could therefore derive q from g_1, dispensing with g_2 altogether.

A modified Golay pair is presented in figure 7. The second code of the pair is complex and thus both real and imaginary values are plotted. The autocorrelations are plotted underneath each code. Observe that the autocorrelation of the modified code is purely imaginary at nonzero lag. When squared, these imaginary values become negative. The sum of squared autocorrelations thus cancel to produce a delta function.

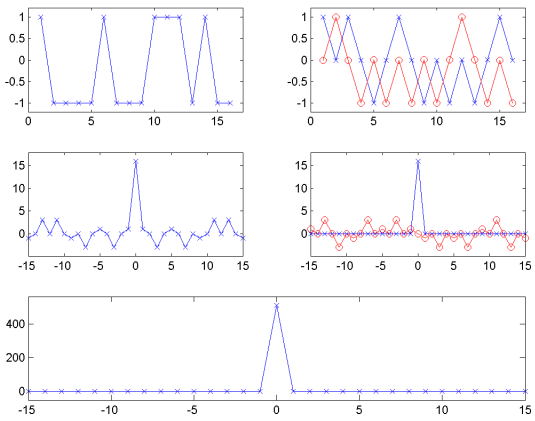

Fig. 7. Modified Golay pair, autocorrelations, and sum of squared autocorrelations

3) Modified Golay code pair derived from frequency domain: Let $g_1(n)$ and $g_2(n)$ be a Golay complementary pair of length N. Then

$$R_{g_1}(k) + R_{g_2}(k) = 2N\delta(k) \tag{47}$$

From the Weiner–Khintchine theorem,

$$S_{g_1}(f) + S_{g_2}(f) = 2N \tag{48}$$

It has been shown [15] that if $g_1(n)$ is a Golay sequence then $g_1(n)e^{i\pi n}$ is complementary with $g_2(n)e^{i\pi n}$. However if the codes are of standard construction and have length 2^m then each code can be expressed

as the interleaving a Golay pair of length 2^{m-1}.

$$g_1(n) = [a(0), b(0), a(1), b(1), a(2), b(2), \cdots] \tag{49}$$

It is known [16] that $g_1(n)$ is complementary with $\tilde{g}_1(n)$,

$$\begin{aligned} \tilde{g}_1(n) &= [a(0), -b(0), a(1), -b(1), a(2), -b(2), \cdots] \\ &= g_1(n)e^{i\pi n} \end{aligned} \tag{50}$$

that is, $g_1(n)$ is complementary with $g_1(n)e^{i\pi n}$. We note that this property also follows from consideration of eq. (39). Therefore

$$S_{g_1}(f) + S_{g_1}(f - \pi) = 2N \tag{51}$$

$$S_{g_1}(f - \pi) = S_{g_2}(f) \tag{52}$$

We require two sequences $q_1(n)$ and $q_2(n)$ whose squares are complementary, that is

$$R^2_{q_1}(k) + R^2_{q_2}(k) = 2N^2\delta(k) \tag{53}$$

From the windowing property of the Fourier transform,

$$(S_{q_1} * S_{q_1})(f) + (S_{q_2} * S_{q_2})(f) = 2N^2 \tag{54}$$

where $*$ denotes convolution. We note that the original Golay sequences g_1 and g_2 are unsuitable because

$$R^2_{g_1}(k) = R^2_{g_2}(k) \tag{55}$$

Consider the frequency shifted convolution

$$\begin{aligned} (S_{g_1} * S_{g_1})(f - \pi) &= \sum_{x=-\infty}^{\infty} S_{g_1}(x) S^*_{g_1}(f - \pi - x) \\ &= \sum_{x=-\infty}^{\infty} (2N - S_{g_1}(x - \pi)) S^*_{g_1}(f - \pi - x) \\ &= \sum_{x=-\infty}^{\infty} 2N S^*_{g_1}(f - \pi - x) - \sum_{x=-\infty}^{\infty} S_{g_1}(x - \pi) S^*_{g_1}(f - \pi - x) \\ &= 2N^2 - (S_{g_1} * S_{g_1})(x) \end{aligned} \tag{56}$$

So the frequency shift property of (51) is preserved by taking self–convolutions. Taking inverse Fourier transforms and rearranging,

$$R^2_{g_1}(k) + e^{i\pi k} R^2_{g_1}(k) = 2N^2\delta(k) \tag{57}$$

Note that one could substitute R_{g_2} for R_{g_1} in either or both of the terms above due to (55). We may thus choose

$$q_1(n) = g_1(n) \qquad \text{or} \quad q_1(n) = g_2(n) \tag{58}$$

and

$$q_2(n) = g_1(n)e^{i\frac{\pi}{2}n} \quad \text{or} \quad q_2(n) = g_2(n)e^{i\frac{\pi}{2}n} \tag{59}$$

in order to satisfy (57).

IV. Use of the Modified Golay Pair

A. Updated signal model

$g_1(n)$ and $g_2(n)$ form a Golay pair of length $N = 2^x$. $g_1(n)$ is used to phase modulate a radar pulse at carrier ω_c. The polyphase code $q(n)$ is derived from $g_2(n)$ by

$$q(n) = g_2(n)e^{i\frac{\pi}{2}n} \tag{60}$$

and is used to modulate radar pulses above and below carrier at $\omega_c + \omega_f$ and $\omega_c - \omega_f$. The transmitted signal is thus

$$s_m(t) = b_g(t)e^{i\omega_c t} + b_q(t)e^{i(\omega_c+\omega_f)t} + b_q(t)e^{i(\omega_c-\omega_f)t} \tag{61}$$

where $b_g(t)$ and $b_q(t)$ are the continuous baseband modulated versions of $g_1(n)$ and $q(n)$ respectively, as defined in (1).

This is reflected from M targets, each with delay d_i, radial velocity v_i and complex attenuation A_i, $i = 1 \dots M$. The signal measured at the receiver is thus

$$\begin{aligned} \tilde{s}_m(t) = \sum_{j=1}^{M} \; & A_j b_g(t-d_j)e^{i\omega_c(1+\frac{2v_j}{c})t}e^{-i\omega_c d_j} \\ & + A_j b_q(t-d_j)e^{i(\omega_c+\omega_f)(1+\frac{2v_j}{c})t}e^{-i(\omega_c+\omega_f)d_j} \\ & + A_j b_q(t-d_j)e^{i(\omega_c-\omega_f)(1+\frac{2v_j}{c})t}e^{-i(\omega_c-\omega_f)d_j} \end{aligned} \tag{62}$$

The returned signal is downmixed and filtered in order to produce three baseband signals

$$\tilde{b}_0(t) = \sum_{j=1}^{M} A_j b_g(t-d_j) e^{i\psi_{0,j}t} e^{-i\omega_c d_j} \tag{63}$$

$$\tilde{b}_1(t) = \sum_{j=1}^{M} A_j b_q(t-d_j) e^{i\psi_{1,j}t} e^{-i(\omega_c+\omega_f) d_j} \tag{64}$$

$$\tilde{b}_{-1}(t) = \sum_{j=1}^{M} A_j b_q(t-d_j) e^{i\psi_{-1,j}t} e^{-i(\omega_c-\omega_f) d_j} \tag{65}$$

where $\psi_{f,j}$ is the Doppler term for the jth return at frequency offset $f\omega_f$, i.e.

$$\psi_{f,j} = (\omega_c + f\omega_f)\frac{2v_j}{c} \tag{66}$$

Each of the downmixed signals is cross–correlated with its corresponding baseband waveform. This is equivalent to computing the zero–Doppler slice of the cross–ambiguity function.

$$\xi_0(\tau) = \sum_{j=1}^{M} A_j e^{-i\omega_c d_j} e^{i(\psi_{j\,0} d_j)} \chi_{b_g}(\tau - d_j, -\psi_{0,j}) \tag{67}$$

$$\xi_1(\tau) = \sum_{j=1}^{M} A_j e^{-i\omega_c d_j} e^{i(\psi_{j\,1} d_j - \omega_f d_j)} \chi_{b_q}(\tau - d_j, -\psi_{1,j}) \tag{68}$$

$$\xi_{-1}(\tau) = \sum_{j=1}^{M} A_j e^{-i\omega_c d_j} e^{i(\psi_{j\,-1} d_j + \omega_f d_j)} \chi_{b_q}(\tau - d_j, -\psi_{-1,j}) \tag{69}$$

B. Single stationary target

In this case $M = 1$ and $v_1 = 0$. The three cross–correlation equations reduce to

$$\xi_0(\tau) = Ae^{-i\omega_c d} \chi_{b_g}(\tau - d, 0) \tag{70}$$

$$\xi_1(\tau) = Ae^{-i\omega_c d} e^{i(\omega_f(\tau-d))} \chi_{b_q}(\tau - d, 0) \tag{71}$$

$$\xi_{-1}(\tau) = Ae^{-i\omega_c d} e^{i(-\omega_f(\tau-d))} \chi_{b_q}(\tau - d, 0) \tag{72}$$

The off–frequency matched filter outputs are multiplied together and added to the square of the centre–frequency output to produce $\Upsilon_0(\tau)$.

$$\begin{aligned}
\Upsilon_0(\tau) &= \xi_0^2(\tau) + \xi_1(\tau)\xi_{-1}(\tau) \\
&= A^2 e^{-i2\omega_c d} \left(\xi_{b_g}^2(\tau - d, 0) + \xi_{b_q}^2(\tau - d, 0) \right) \\
&= A^2 e^{\{\cdot\}} T^2 \left(\chi_\Omega^2 \left(k_1 - \frac{d}{T}, 0 \right) (R_g^2(k_1) + R_q^2(k_1)) + \chi_\Omega^2 \left(k_2 - \frac{d}{T}, 0 \right) (R_g^2(k_2) + R_q^2(k_2)) \right. \\
&\qquad \left. + 2\chi_\Omega \left(k_1 - \frac{d}{T}, 0 \right) \chi_\Omega \left(k_2 - \frac{d}{T}, 0 \right) (R_g(k_1)R_q(k_2) + R_q(k_1)R_g(k_2)) \right)
\end{aligned} \tag{73}$$

where the τ argument has been omitted from k_1 and k_2 for convenience. The third term reduces to zero regardless of the values of k_1 and k_2, due to the autocorrelation properties of the Golay codes. Υ_0 can thus be written

$$\Upsilon_0(\tau) = 2N^2T^2A^2e^{\{\cdot\}}\left(\chi_\Omega^2\left(k_1 - \frac{d}{T}, 0\right)\delta(k_1) + \chi_\Omega^2\left(k_2 - \frac{d}{T}, 0\right)\delta(k_2)\right) \tag{74}$$

Figure 8 gives an example in which a modified Golay–coded signal is transmitted at carrier, while its pair is transmitted at equal and opposite offsets from carrier, and the resulting delayed signal processed to combine the squared cross–ambiguities. The plotted value is the square root of the magnitude of $\Upsilon(\tau)$. Observe that sidelobes have generally been suppressed successfully. What small power remains away

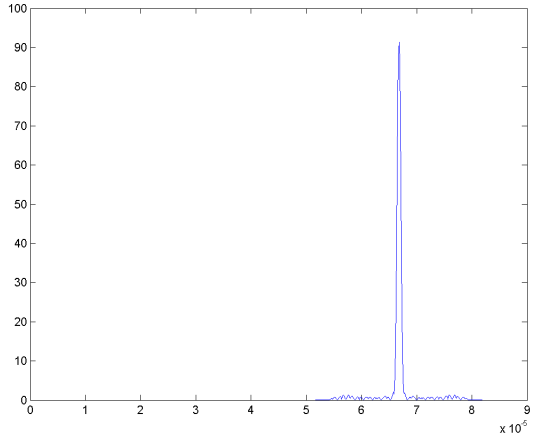

Fig. 8. Result of processing delayed frequency–separated modified Golay–coded signals

from the main lobe is due to nuances of pulse code modulation.

C. Two closely separated stationary targets

In this case $M = 2$, $v_1 = 0$ and $v_2 = 0$. The three matched filter outputs, obtained from eqs. (67–69) by setting Doppler terms to zero, are

$$\xi_0(\tau) = A_1e^{-i\omega_c d_1}\chi_{b_g}(\tau - d_1, 0) + A_2e^{-i\omega_c d_2}\chi_{b_g}(\tau - d_2, 0) \tag{75}$$

$$\xi_1(\tau) = A_1e^{-i(\omega_c+\omega_f)d_1}\chi_{b_q}(\tau - d_1, 0) + A_2e^{-i(\omega_c+\omega_f)d_2}\chi_{b_q}(\tau - d_2, 0) \tag{76}$$

$$\xi_{-1}(\tau) = A_1e^{-i(\omega_c-\omega_f)d_1}\chi_{b_q}(\tau - d_1, 0) + A_2e^{-i(\omega_c-\omega_f)d_2}\chi_{b_q}(\tau - d_2, 0) \tag{77}$$

In this case the quantity $\Upsilon_0(\tau)$ becomes

$$\begin{aligned}\Upsilon_0(\tau) &= \xi_0^2(\tau) + \xi_1(\tau)\xi_{-1}(\tau) \\ &= A_1^2 e^{-i2\omega_c d_1}\left(\chi_g^2(\tau-d_1)+\chi_q^2(\tau-d_1)\right) + A_2^2 e^{-i2\omega_c d_2}\left(\chi_g^2(\tau-d_2)+\chi_q^2(\tau-d_2)\right) \\ &\quad + 2A_1A_2 e^{-i\omega_c(d_1+d_2)}\left(\chi_g(\tau-d_1)\chi_g(\tau-d_2)+\cos(\omega_f(d_2-d_1))\chi_q(\tau-d_1)\chi_q(\tau-d_2)\right)\end{aligned} \tag{78}$$

where $\xi(\tau) = \xi(\tau, 0)$ and $\chi(\tau) = \chi(\tau, 0)$. This contains two terms similar to (74), one for each target. The third term is due to cross–terms which arise from the squaring operation. Sidelobes are suppressed only at the cost of introducing these multi–target cross–terms. When $|d_1 - d_2| < 2NT$ there is no overlap and the cross–terms vanish. When the relative delay is an odd number of chips, $\delta_d = (2k+1)T$, then cross–terms away from the mainlobe are mitigated by the relative positions of zeros in the autocorrelation functions. If the delay is an even number of chips, $\delta_d = 2kT$, Then the two terms in $\chi(\tau)$ will cancel upon addition provided that the cosine factor evaluates to ± 1 as appropriate. This will be the case when the offset frequency ω_f is chosen such that

$$2T\omega_f = (2k+1)\pi \tag{79}$$

When the delay is not a whole number of chips, cancellation of the sidelobes does not occur due to the magnitude of the cosine term being less than one. For a hypothesised distance δ_d it is possible to compute the value of ω_f which forces the cosine factor to ± 1, thereby minimising the cross–terms away from the main lobes. This can be computed as

$$\tilde{\omega}_f = \frac{\arccos(\text{sign}(\cos(\frac{\pi\delta_d}{2T}))) + k2\pi}{\delta_d} \tag{80}$$

This will minimise the power of cross–terms away from the main lobes. Some cross term power will remain if δ_d is not a whole number of chips. However one notes that cross term power is a periodic function of the offset frequency, and that choosing an offset of $\tilde{\omega}_f + \pi$ will cause nulls to occur where previously there were peaks. The magnitude of $\chi(\tau)$ for two arbitrary closely seperated targets is presented in figure 9 as a function of τ and ω_f. Observe that the cross–terms are strongest in the vicinity of the main lobes. Observe that the cross–terms are indeed periodic with respect to ω_f. One of the values suitable for ω_f as computed by eq. (80) is indicated by a white dashed line. Observe that this value of ω_f produces the smallest off–peak cross–terms, but that some narrow subpeaks still remain. The frequency $\omega_f + \pi$ is indicated with a white dashdot line. Observe that the nulls occur at the positions in which narrow sub-peaks occur at ω_f. This suggests a multiple–pulse cross term suppression regime. Detections made in one PRI may be used to design the offset frequency for the next PRI, in order to minimise cross–terms from the hypothesised targets.

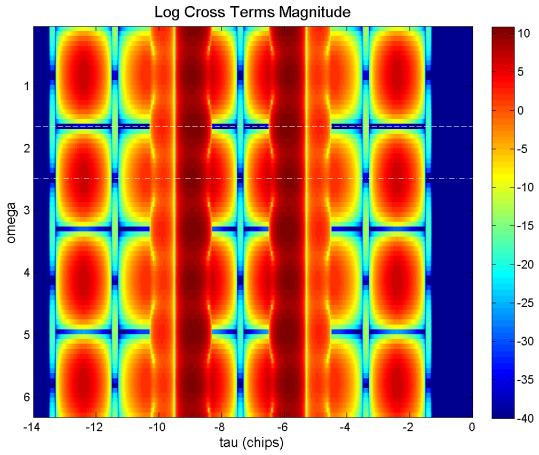

Fig. 9. cross–terms log–magnitude

1) Comparison with Frank code: Consider a situation in which there are two stationary reflectors, one returning power 20 dB lower than the other. Furthermore the smaller return is located at a range which locates it within a sidelobe of the stronger return when interrogated with a Frank coded waveform. A plot of matched filter magnitude for such a scenario is presented in figure 10. The position of each target

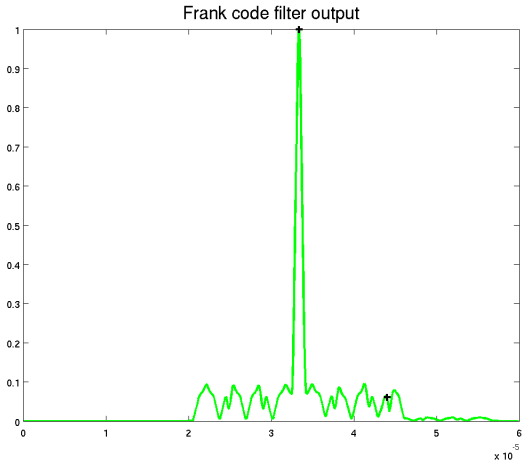

Fig. 10. Matched filter magnitude, two returns, Frank coded waveform

is marked with a cross. Note that the effect of the weaker target on the filter output is to cause a slight perturbation in the sidelobe magnitude of the stronger target. This is not easily detectable by eye.

Consider the same scenario interrogated with the frequency separated modified Golay codes as de-

scribed previously. The square root of $\Upsilon_0(\tau)$, the combined matched filter outputs, is plotted in figure 11. Observe that in this filter output the weaker target is quite visible. cross–terms are also visible but of a

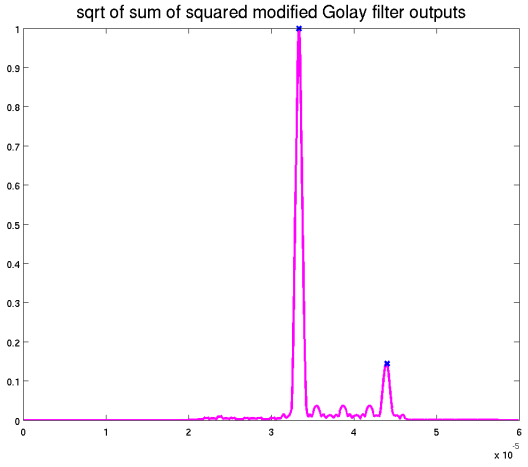

Fig. 11. Combined matched filter magnitude, two returns, frequency separated modified Golays

magnitude far smaller than the second return.

It must be noted that the cross–terms may reinforce or impede the response to the second target, depending upon their relative phase. The cross term has not been detrimental in this case. The effect of cross–terms depends upon the underlying Golay codes and the offset frequency as well as the distance between the targets. For certain combinations of parameters the results will not be as clement. However the choice of Golay codes and the offset frequency may be varied, thus allowing some control over the cross–terms.

2) Simulations: The degree to which a secondary return is hidden by off–centre cross–terms due to a stronger return depends upon the precise seperation of the two returns, and also the phase change incurred by reflection (radar cross section). In some cases the return power will be reinforced, in other cases it will be impeded. The maximum interpeak cross–term magnitude will occur when the separation $d_2 - d_1$ brings the two largest sidelobes of the individual codes into alignment, and also when the offset frequency ω_f is such that the cosine term in eq. (78) becomes equal to 1. Note that this is the maximum possible value in between the signal returns; the cross–term contribution may be higher at the true return positions. For the length–16 Golay codes used in this study the maximum off–centre cross–correlation value is 3, and thus the maximum possible off–target cross–term magnitude becomes

$$X_\Upsilon = 2A_1A_2\left|3 \times 3 + 3 \times 3\right| \tag{81}$$

Any secondary target should be detectable in the presence of cross–terms provided that it exceeds this value.

The maximum sidelobe level of a length–N Frank code, and also a Px code, is given in [17] as $\left(\sin\frac{\pi}{\sqrt{N}}\right)^{-1}$. For a 16–Frank coded return of peak amplitude A the maximum sidelobe level in the matched filter output is thus

$$X_F = \sqrt{2}A \tag{82}$$

The length–16 Minimum Peak Sidelobe (MPS) code [17] has a maximum sidelobe level of 2. The maximum sidelobe level in matched filter output is therefore

$$X_M = 2A \tag{83}$$

Any secondary target should be detectable in the presence of sidelobes provided that it exceeds the maximum sidelobe level for the type of pulse coding used.

Simulations were performed in which a return from two closely spaced targets was simulated. The weaker return had one hundredth of the power of the stronger return. In each simulation the distance separating the returns was chosen at random, as was the complex reflection coefficient (radar cross section). Signals were generated according to the modified Golay code method and nonlinear processing performed to recover $\Upsilon(\tau)$. The local maximum closest to the known location of the second, weaker return was found and compared to a threshold computed as the maximum expected off–centre cross–term level, eq. (81). If the nearest local maximum exceeded this level then the secondary peak was deemed to be detectable. Signals were also generated by pulse coding with length–16 Frank codes, Px codes and MPS codes. In each case the matched filter output was computed and the local maximum in the vicinity of the second weak return was compared to the theoretical maximum sidelobe level. 1000 simulations were performed and the results presented in table I. The secondary peak was detectable in almost every simulation when the nonlinear modified–Golay method was used. This was not the case with simple pulse–code modulation. The secondary target remained undetectable in about 15% of simulations when Px coding was used, as was undetectable in two–thirds of simulations when MPS binary coding was used.

These results demonstrate the superiority of the nonlinear modified–Golay method to resolve targets in clutter. Sidelobes inherent in pulse–coding schemes are replaced by cross–terms. However these cross–terms are small as they depend upon the power of the secondary return, and manageable as they depend upon the chosen offset frequency. It has been demonstrated that the cross–terms generally do not conceal

method	# secondary dets
mod. Golay	993
Frank	735
Px	851
MPS binary	339

TABLE I

COUNT OF DETECTABLE SECONDARY WEAK RETURNS

the presence of secondary weak targets. Indeed the presence of cross–terms is indicative of the presence of a secondary target, because an isolated return produces a single spike in the processor output.

D. Moving target

Consider the case where two targets are present ($M = 2$), each with amplitude A_i and possibly nonzero velocity v_i. In this case the output of the matched filters at nonzero Doppler are of interest. The outputs can be written as

$$\xi_0(\tau,\phi) = A_1 e^{-i\omega_c d_1}\chi_{b_g}(\tau - d_1, \phi - \psi_{0,1}) + A_2 e^{-i\omega_c d_2}\chi_{b_g}(\tau - d_2, \phi - \psi_{0,2}) \tag{84}$$

$$\xi_1(\tau,\phi) = A_1 e^{-i(\omega_c+\omega_f) d_1}\chi_{b_q}(\tau - d_1, \phi - \psi_{1,1}) + A_2 e^{-i(\omega_c+\omega_f) d_2}\chi_{b_q}(\tau - d_2, \phi - \psi_{1,2}) \tag{85}$$

$$\xi_{-1}(\tau,\phi) = A_1 e^{-i(\omega_c-\omega_f) d_1}\chi_{b_q}(\tau - d_1, \phi - \psi_{-1,1}) + A_2 e^{-i(\omega_c-\omega_f) d_2}\chi_{b_q}(\tau - d_2, \phi - \psi_{-1,1}) \tag{86}$$

The precise Doppler offsets for a particular at each frequency are similar as $v_i << c$ and $\omega_f << \omega_c$. Therefore make the approximation

$$\psi_{m,i} \approx \psi_{0,i} \;\; m \in \{-1, 0, 1\} \tag{87}$$

For notational convenience the first subscript is dropped.

The output of the nonlinear processing can thus be written as

$$\begin{aligned}\Upsilon(\tau,\phi) = {} & A_1^2 e^{-i2\omega_c d_1}\left[\chi^2_{b_g}(\tau - d_1, \phi - \psi_1) + \chi^2_{b_q}(\tau - d_1, \phi - \psi_1)\right] \\ & + A_2^2 e^{-i2\omega_c d_2}\left[\chi^2_{b_g}(\tau - d_2, \phi - \psi_2) + \chi^2_{b_q}(\tau - d_2, \phi - \psi_2)\right] \\ & + \begin{array}{r} 2A_1A_2 e^{-i\omega_c(d_1+d_2)}\left[\chi_{b_g}(\tau - d_1, \phi - \psi_1)\chi_{b_g}(\tau - d_2, \phi - \psi_2)\right. \\ \left. + \cos\omega_f(d_1 - d_2)\;\chi_{b_q}(\tau - d_1, \phi - \psi_1)\chi_{b_q}(\tau - d_2, \phi - \psi_2)\right] \end{array}\end{aligned} \tag{88}$$

This is similar in form to eq. (78). Each target should form a spike along the line specified by $\phi = \psi_i$. Cross–terms will again be large at the target locations due to the strong responses of the χ components at these locations, but cross–terms will persist at interpeak locations. Much power will be present at the correct propagation delays on the zero Doppler axis due to the expected target velocities being much lower than the propagation velocity. However the propagation delays d_i are a function of time,

$$d_i(t) = d_i(0) + v_i t \tag{89}$$

Observe that the phase of the target terms in Υ is dependent wholly upon the delay to that target,

$$\varphi_i(t) = 2\omega_c d_i \tag{90}$$

However the phase on the cross–terms is equal to the average of these terms,

$$\varphi_x(t) = \omega_c(d_1 + d_2) \tag{91}$$

So the cross–terms change at a different frequency from that of either target. Note also that the squaring operation results in the target terms being shifted by twice the Doppler frequency.

Interpulse Doppler processing can be performed by computing the zero–Doppler slice of the nonlinear processor output from K consecutive pulses, $\Upsilon_k(\tau, 0), \;\; 1 \leq k \leq K$, and computing the Fourier transform across the pulses at each delay.

A scenario having two closely–spaced returns of equal power was simulated. The first target had a velocity of 2 m/s, the second had velocity 20 m/s. Returns from the targets in 64 consecutive pulse intervals were simulated and processed to compute $\Upsilon(\tau, 0)$. The magnitudes of Υ are presented as an image in figure 12. Pulse Doppler processing was performed on the recorded Υ vectors by performing a Fourier transform over the pulses on the data in each range bin. The magnitude of the result is given in figure 13. Observe that the two targets have been resolved in Doppler as well as range. Further observe that the cross–terms appear at a frequency between that of the main target terms.

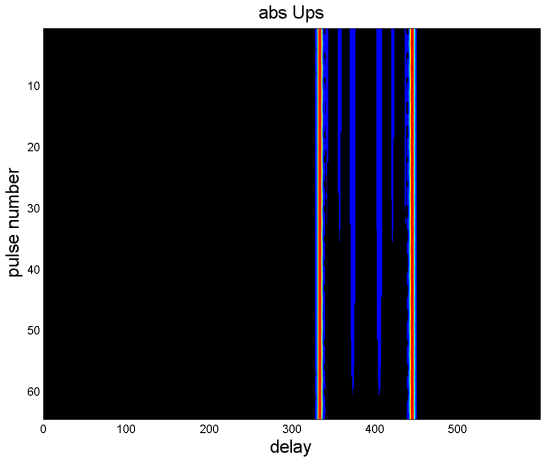

Fig. 12. $\Upsilon(\tau, 0)$ in 64 consecutive pulse intervals

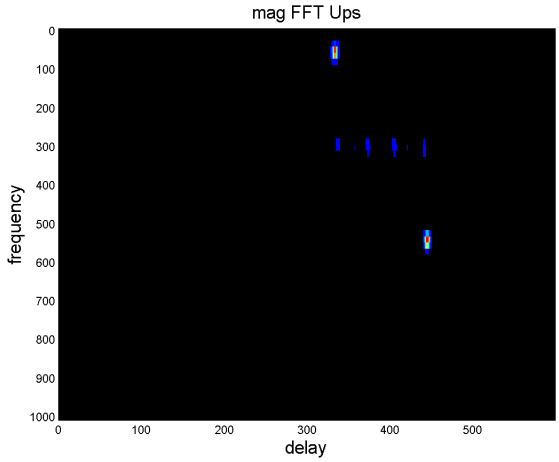

Fig. 13. Result of pulse Doppler processing on Υ

V. Noise issues

Although the nonlinear processing method is designed for clutter suppression, and so far noise has been assumed to be absent, it is necessary to consider the effect of noise on the scheme. Assume that the received signal $\tilde{s}_m(t)$ (eq. 62) contains a single return from a target, and also contains additive Gaussian

noise. This signal is downmixed and lowpass filtered to produce three component signals

$$\tilde{b}_0(t) = Ab_g(t-d)e^{i\psi_0 t}e^{-i\omega_c d} + n_0(t) \tag{92}$$

$$\tilde{b}_1(t) = Ab_q(t-d)e^{i\psi_1 t}e^{-i(\omega_c+\omega_f)d} + n_1(t) \tag{93}$$

$$\tilde{b}_{\bar{1}}(t) = Ab_q(t-d)e^{i\psi_{\bar{1}} t}e^{-i(\omega_c-\omega_f)d} + n_{\bar{1}}(t) \tag{94}$$

where the $n_x(t)$ terms are band–limited noise sequences. The spectrum of these sequences will be shaped by the lowpass filter, however assume for simplicity that these are ideally shaped (flat) within the passband.

A. *Effect of noise on* Υ

Matched filter outputs of the noisy component signals can be expressed in terms of the noise–free outputs (eq. 67–69)

$$\xi_{n_0}(\tau) = \xi_0(\tau) + X(\tau) \tag{95}$$

$$\xi_{n_1}(\tau) = \xi_1(\tau) + Y(\tau) \tag{96}$$

$$\xi_{n_{\bar{1}}}(\tau) = \xi_{\bar{1}}(\tau) + Z(\tau) \tag{97}$$

Where the X, Y and Z are noise processes, each formed by the filtering of a noise term $n_i(t)$ with a Golay–coded pulse sequence. Since the Golay codes have relatively flat spectra, the filtered noise sequences also have relatively flat spectra, and are thus approximately complex Gaussian distributed, $X(\tau), Y(\tau), Z(\tau) \sim N_C(0, \sigma_z^2)$, so σ_z^2 is the noise power at the filter output. The sum of squared filter outputs for the noisy signal is thus

$$\Upsilon_n(\tau) = \xi_{n_0}^2(\tau) + \xi_{n_1}(\tau)\xi_{n_{\bar{1}}}(\tau) \tag{98}$$

$$\begin{aligned} =&\xi_0^2(\tau) + 2\xi_0(\tau)X(\tau) + X^2(\tau) \\ &+ \xi_1(\tau)\xi_{\bar{1}}(\tau) + \xi_1(\tau)Y(\tau) + \xi_{\bar{1}}(\tau)Z(\tau) + Y(\tau)Z(\tau) \end{aligned} \tag{99}$$

$$= \Upsilon(\tau) + \nu(\tau) \tag{100}$$

where $\nu(\tau)$ is a noise term

$$\begin{aligned} \nu(\tau) =& 2\xi_0(\tau)X(\tau) + X^2(\tau) \\ &+ \xi_1(\tau)Y(\tau) + \xi_{\bar{1}}(\tau)Z(\tau) + Y(\tau)Z(\tau) \end{aligned} \tag{101}$$

The power of the noise term is

$$E\left\{\nu(\tau)\nu^*(\tau)\right\} = 4\left|\xi_0(\tau)\right|^2\sigma_z^2 + 2\left|\xi_1(\tau)\right|^2\sigma_z^2 + 2\sigma_z^4 \tag{102}$$

At the sample point corresponding to the actual target delay, $\tau = d$,

$$E\left\{\nu(d)\nu^*(d)\right\} = 6(AT_cN)^2\sigma_z^2 + 2\sigma_z^4 \tag{103}$$

Observe that the expected value of the magnitude of $\Upsilon(\tau)$, given the hypothesis H_1: that a target is present with delay d, is

$$E\left\{\Upsilon(d) \mid H_1\right\} = 2(AT_cN)^2 \tag{104}$$

B. Modified scheme for lower noise variance

Note that the noise contribution from the offset terms is less than that from the non–offset term. The noise power can thus be lessened if the central code is also transmitted simultaneously above and below the central frequency by the same offset. In other words, the single return in eq. (92) is replaced by the two equations

$$\tilde{b}_0(t) = Ab_g(t-d)e^{i\psi_0 t}e^{-i\omega_c d} + n_0(t) \tag{105}$$

$$\tilde{b}_{\bar{0}}(t) = Ab_g(t-d)e^{i\psi_{\bar{0}} t}e^{-i\omega_c d} + n_{\bar{0}}(t) \tag{106}$$

and the matched filter output of eq. (95) is replaced by two matched filters,

$$\xi_{n_0}(\tau) = \xi_0(\tau) + X(\tau) \tag{107}$$

$$\xi_{n_{\bar{0}}}(\tau) = \xi_{\bar{0}}(\tau) + W(\tau) \tag{108}$$

where $W \sim N_C(0, \sigma_z^2)$. In this case the noise term of the nonlinear processor becomes

$$\begin{aligned}\nu(\tau) = \xi_0(\tau)X(\tau) + \xi_{\bar{0}}(\tau)W(\tau) + X(\tau)W(\tau) \\ + \xi_1(\tau)Y(\tau) + \xi_{\bar{1}}(\tau)Z(\tau) + Y(\tau)Z(\tau)\end{aligned} \tag{109}$$

and the noise power reduces to

$$E\left\{\nu(d)\nu^*(d)\right\} = 4(AT_cN)^2\sigma_z^2 + 2\sigma_z^4 \tag{110}$$

at the correct delay $\tau = d$.

C. Noise considerations for a single matched filter detector

The output of a matched filter for a single coded pulse transmitted at carrier is given in eq. (95). In this case the noise term is a complex Gaussian with variance σ_z^2, and the expected value of the magnitude of matched filter output at the correct delay, given the existence of a target, is

$$E\left\{\xi_0(\tau) \mid H_1\right\} = AT_cN \tag{111}$$

However this may not bear comparison with the nonlinear methods described previously due to the fact that less bandwidth is available. The modified nonlinear method uses four pulses, and therefore uses four times the bandwidth. A simple fix is to use a single pulse of the same length but four times the bandwidth. The output of the matched filter depends only on the total energy of the pulse, which is quadrupled by the increase in bandwidth, and in this case the expected value of the magnitude becomes

$$E\left\{\xi_0(\tau) \mid H_1\right\} = 2AT_cN \tag{112}$$

D. ROC evaluation by Monte Carlo simulation

Expressions for probability densities of the noise terms in the nonlinear methods can be found analytically. False alarm probabilities and detection probabilities could be determined by numerical integration of these expressions. However the densities for the magnitudes of the nonlinear quantities are unweildy. For this reason we perform a ROC analysis by Monte Carlo evaluation.

For given values of signal magnitude A and noise power σ_z^2 at the output of the matched filters, a noise term ν is simulated according to eq. (101). The magnitude of ν is compared with a threshold and, if greater, a false alarm is recorded. The magnitude of $\nu + E\left\{\Upsilon\right\}$ is compared with the same threshold and, if greater, a detection is recorded. This is performed over a large number of trials, and the counts are divided by the number of trials to obtain Monte Carlo estimates of false alarm and detection probabilities. This method is performed over a range of different thresholds and the results plotted as a Receiver–Operator Curve.

ROCs for the modified nonlinear method, a single matched filter and a higher–bandwidth matched filter are computed in an analagous manner, simply substituting the correct expressions for noise and expected magnitude as appropriate.

Figure 14 shows ROC curves generated for a single–pulse matched filter detector, a matched–filter detector of four times the bandwidth, the original nonlinear detector (only one code doubly offset), and the modified nonlinear detector (both codes doubly offset). In this example the SNR at the output of the matched filter was 0 dB. Observe that the high–bandwidth matched filter detector is best performed, which is to be expected since this is optimal in Gaussian noise. However both nonlinear methods outperform the single–pulse matched filter of low bandwidth. As expected the modified nonlinear method outperforms the original formulation, due to the better suppression of noise.

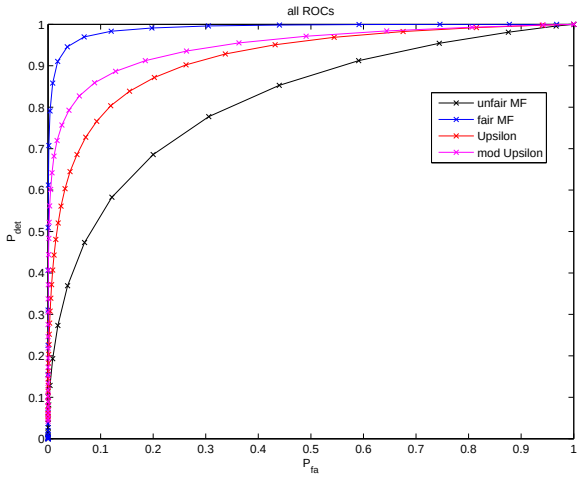

Fig. 14. ROC curves for four detection methods

VI. Conclusion

It has been shown that seperation of a code pair in frequency destroys its complementarity, as the unknown delay causes unknown changes in phase, preventing coherent combination. However it is shown how the relative phase differences may be overcome by offsetting the second code equally above and below the first. This causes offset–related phase differences to cancel when the two matched filter outputs are multiplied together. The sum of squared matched filter outputs may thus be recovered.

A code pair exhibiting complementary behaviour in the square has been derived by modification of one sequence of a length–2^x Golay pair. This modified code pair used in conjuction with equal and opposite frequency offsetting has been shown to achieve sidelobe–free filter output.

The chief tradeoff in the achievement of complementary behaviour is the introduction of cross–terms when two or more returns are closely seperated. However the effect of cross–terms is dependent upon offset frequency, among other factors, and may thus be controlled. In spite of the presence of cross–terms the method has been demonstrated to locate small returns in situations where a Frank coded pulse could not.

The effects of noise on the algorithm are amplified by the nonlinear squaring operation. This can be partly mitigated by transmitting both codes offset above and below the carrier. ROC analysis indicates that the nonlinear methods provide a greater probability of detection for a given false alarm rate compared with the case when one of the pulses is used as a simple matched filter detector. However detection performance is below that of a matched filter of bandwidth equivalent to the total used by the four

seperated pulses. It must be remembered here that this scheme is designed to be used in clutter limited applications and not noise limited ones.

APPENDIX

FILTERING OF SIDELOBES WITH A SINGLE CODE

A further property of the modified code is that the main lobe of its autocorrelation is out of phase with its sidelobes. A simple eigendecomposition algorithm may be employed for isolation of the main lobe. This algorithm is mostly applicable in situations where there is only one return, which is not generally the case in radar returns. However this algorithm may find application to other problems such as synchronisation in mobile telephony.

The autocorrelation of the sequence q

$$R_q(k) = e^{i\frac{\pi}{2}k} R_{g_2}(k) \tag{113}$$

Since R_{g_2} is real valued for all k, and is zero valued at all even lags except $k = 0$, it follows that

$$\Re\{R_q(k)\} > 0, \quad \text{if } k = 0 \tag{114}$$

$$\Re\{R_q(k)\} = 0, \quad \text{if } k \neq 0 \tag{115}$$

In other words, the off–centre values of the autocorrelation of q sequence are purely imaginary. When q is used to modulate a radar pulse, the sidelobes in the filtered response will be out of phase with the main lobe by $\frac{\pi}{2}$ radians. This fact may be exploited to separate the main lobe from the sidelobes.

Consider equation (71) which is the matched filter response of the signal component downmodulated from $\omega_c + \omega_f$, which was encoded with q.

$$\xi_1(\tau) = Ae^{i(\omega_c+\omega_f)(\tau-d)} \chi_{b_q}(\tau - d, 0) \tag{116}$$

Define a two dimensional vector–valued function $\boldsymbol{\zeta}$ as

$$\boldsymbol{\zeta}(\tau) = \left(\Re\{\xi_1(\tau)\}, \Im\{\xi_1(\tau)\}\right)^T \tag{117}$$

Further define Z, the covariance matrix of $\boldsymbol{\zeta}$, as

$$Z = E\left\{\boldsymbol{\zeta}\, \boldsymbol{\zeta}^H\right\} \tag{118}$$

Performing an eigendecomposition on Z,

$$Z = V \Lambda V^H \tag{119}$$

where V is a 2 by 2 matrix of eigenvectors of Z and Λ a diagonal matrix of the 2 eigenvalues.

$$V = (\boldsymbol{v}_1, \boldsymbol{v}_2) \tag{120}$$

$$\Lambda = \begin{pmatrix} \lambda_1 & 0 \\ 0 & \lambda_2 \end{pmatrix} \tag{121}$$

Assume that $\lambda_1 > \lambda_2$. Since most of the matched filter output power forms the main lobe, v_1 is the eigenvector corresponding to the main lobe, and the relationship of its two component elements is a function of the unknown phase term on the main lobe.

The signal can be separated into mainlobe and sidelobe components by projection onto the spaces described by the two eigenvectors.

$$z_{\text{main}}(\tau) = \boldsymbol{\zeta}(\tau)^T \boldsymbol{v}_1 \tag{122}$$

$$z_{\text{side}}(\tau) = \boldsymbol{\zeta}(\tau)^T \boldsymbol{v}_2 \tag{123}$$

The ability of this method to isolate the main lobe will be hampered by noise and also by the presence of other returns.

An example of a delayed modified Golay return and the magnitude of its cross–correlation with the original baseband modified Golay signal are given in figure 15. The results of processing the matched

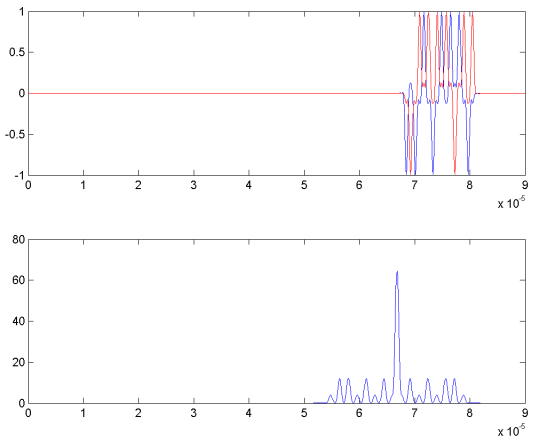

Fig. 15. One modified Golay signal and its cross–correlation

filter output with the eigenseparation algorithm is presented in figure 16. Observe that the signal has been successfully separated into mainlobe and sidelobe components.

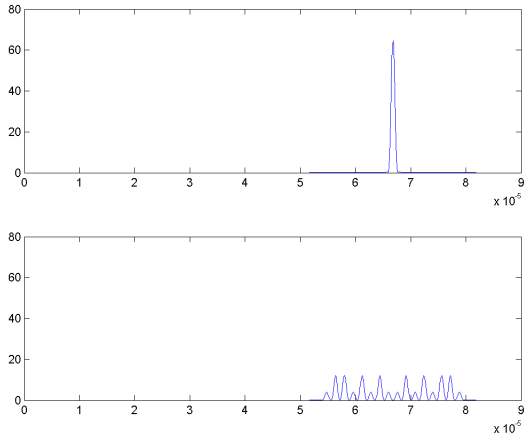

Fig. 16. Projection of modified Golay signal onto mainlobe and sidelobe spaces

REFERENCES

[1] R. Barker, "Group synchronizing of binary digital sequences," *Comm. Theory, London, Butterworth*, pp. 273–287, 1953.

[2] R. L. Frank, "Polyphase complementary codes," *IEEE trans. Info. Theory*, vol. 26, pp. 641–647, November 1980.

[3] P. Rapajic and R. Kennedy, "Merit factor based comparison of new polyphase sequences," *IEEE Communication Letters*, vol. 2, pp. 269–270, October 1998.

[4] J. Mittermayer and J.M.Martinez, "Analysis of range ambiguity suppression in SAR by up and down chirp modulation for point and distributed targets," in *Proc. IEEE Intl. Geoscience and Remote Sensing Symposium*, vol. 6, pp. 4077–4079, July 2003.

[5] F. Robey, S. Coutts, D. Weikle, J. McHarg, and K. Cuomo, "MIMO radar theory and experimental results," in *in 38th Asilomar Conf. on Signals Systems and Computers*, vol. 1, pp. 300–304, 2004.

[6] J-C. Guey and M. R. Bell, "Diversity waveform sets for delay–Doppler imaging," *IEEE trans. Info. Theory*, vol. 44, pp. 1504–1522, 1998.

[7] C. Chang and M. Bell, "Frequency division multiplexing technique for composite ambiguity function approximation," in *Defence Applications of Signal Processing*, 2005.

[8] S. Suvorova, B. Moran, E. Kalashyan, P. Zulch, and R. Hancock, "Radar performance of temporal and frequency diverse phase-coded waveforms," in *2nd Intl. Waveform Diversity & Design Conference, Hawaii USA*, 2006.

[9] S-M. Tseng, D-F. Tseng, G-F. Huang, Y. C. Tzeng, and W-C. Tseng, "Realization of diversity waveform sets for delay–Doppler imaging," in *IEEE Asia–Pacific Conf. on Circuits and Systems, Dec. 6–9*, pp. 237–240, 2004.

[10] M. Parker, K. Paterson, and C. Tellambura, "Golay complementary sequences," in *Wiley Encyclopedia of Telecommunications* (J. G. Proakis, ed.), Wiley, 2003.

[11] A. Pezeshkia, A. R. Calderbank, W. Moran, and S. Howard, "Doppler resilient waveforms with perfect autocorrelation," *Submitted to IEEE Trans. Info. Theory*, 2007.

[12] M. Richards, *Fundamentals of radar signal processing*. McGraw-Hill, 2005.

[13] H. van Trees, *Radar–Sonar Signal Processing and Gaussian Signals in Noise (Detection Estimation and Modulation Theory part III)*. Wiley-Interscience, 1968.

[14] Y. Taki, H. Miyakawa, M. Hatori, and S. Namba, "Even–shift orthogonal sequences," *IEEE transactions on Information Theory*, vol. 15, no. 2, pp. 295–300, 1969.

[15] S. Budišin, "Golay complementary sequences are superior to PN sequences," in *IEEE International Conference on Systems Engineering, Kobe*, pp. 101–104, September 1992.

[16] R. Urbanke and A. S. Krishnakumar, "Compact description of Golay sequences and their extensions," in *Proc. 34th Annual Allerton Conf. Communication, Control and Computing*, pp. 693–702, University of Illinois, 1996.

[17] N. Levanon and E. Mozeson, *Radar Signals*. Wiley, 2004.